

Deviation from exponential decay for spin waves excited with a coplanar waveguide antenna

Daniel R. Birt,^{1,2} Kyongmo An,² Maxim Tsoi,^{1,2} Shingo Tamaru,³ David Ricketts,³ Kin L. Wong,⁴ Pedram Khalili Amiri,⁴ Kang L. Wang,⁴ and Xiaoqin Li^{1,2,a)}

¹Texas Materials Institute, The University of Texas at Austin, Austin, Texas 78712, USA

²Department of Physics, Center for Nano- and Molecular Science and Technology, The University of Texas at Austin, Austin, Texas 78712, USA

³Electrical and Computer Engineering Department, Carnegie Mellon University, Pittsburgh, Pennsylvania 15213, USA

⁴Department of Electrical Engineering, University of California, Los Angeles, California 90095, USA

(Received 9 August 2012; accepted 5 December 2012; published online 20 December 2012)

We have investigated the propagation of surface spin waves in a Permalloy thin film excited by an asymmetric coplanar antenna. A surprising oscillatory behavior superimposed on the exponential decay is observed in the spin wave intensity mapped with the micro-Brillouin light scattering technique. The oscillations can be modeled as the interference between a propagating spin wave and a background magnetization with spatially uniform phase. We use a simple closed-form equation that includes both contributions to fit our experimental results. From the fit results, we extract the spin wave propagation length and the spin wave vector in a frequency range limited by the antenna bandwidth. © 2012 American Institute of Physics. [<http://dx.doi.org/10.1063/1.4772798>]

The continuing demands of advancing information storage and processing technologies have attracted much attention to spin waves in magnetic microstructures.¹ Numerous experiments have demonstrated that spin waves play an important role in the operation of spin torque based memory devices^{2,3} and spin torque nanoscillators.^{4,5} In addition, several spintronic devices based on propagating spin waves have been proposed, such as the spin wave bus⁶ and a Mach Zehnder-type interferometer for performing logic operations.⁷ A key parameter that affects the design of such devices is the spin wave propagation length, which is defined as the distance the spin wave propagates before the amplitude decays by e^{-1} . In magnetic insulators such as yttrium iron garnet (YIG), the propagation length is rather long, on the order of millimeters. In metals such as Permalloy (Py, Ni₈₀Fe₂₀), the propagation length is significantly reduced to just a few microns or tens of microns, making the basic task of determining the propagation length challenging.

Several measurement techniques can be used to determine the propagation length. One method, known as propagating spin wave spectroscopy, involves only electrical signals.^{8–10} Spin waves are excited with a coplanar waveguide antenna and the signal is detected some distance away with another antenna through inductive coupling. The spatial spin wave intensity profile could be measured using a series of devices with different spacing between the excitation and detection antennas. There are several drawbacks to this approach including a large background signal from direct inductive coupling, variations between devices, and limited spatial resolution. Optical spectroscopic methods, such as Magneto-optic Kerr Effect (MOKE) microscopy¹¹ or micro-Brillouin light scattering microscopy (micro-BLS),¹² are more suitable for characterizing spin wave propagation

lengths due to their high spatial resolution (~ 300 nm) and ability to scan position conveniently. We have chosen micro-BLS because the detector does not need to be synchronized to the excitation source. This flexibility allows us to easily scan the excitation frequency.

In this report, we investigated the propagation of magnetostatic surface spin waves (MSSW) in a continuous Py thin film excited by an asymmetric coplanar waveguide antenna. The spin waves were excited in the Damon-Eshbach¹³ configuration, wherein a static magnetic field was applied parallel to the antenna and perpendicular to the propagation direction of the spin waves. While mapping the spatial dependence of the surface spin wave intensity, we observed a significant deviation from the simple exponential decay due to damping: an oscillatory signal is superimposed on top of the exponential decay. To model the observed complicated spatial dependent spin wave intensity, we use a closed-form expression that includes contributions from the propagating spin wave and a background magnetization with spatially uniform phase. This simplified closed-form model allows us to fit the experimental data and to extract several key parameters including the wave vectors, the group velocities, and the propagation lengths of the excited spin waves.

The device studied consists of a nominally 40-nm-thick Py film sputtered on a silicon substrate. The Py film is covered with a 240-nm-thick layer of SiO₂, which isolates the film electrically from the antenna. An asymmetric coplanar waveguide antenna was defined using photolithography and fabricated by thermal deposition of 300 nm of gold. The antenna consists of a 12- μ m-wide signal line connected to a 6- μ m-wide ground line with a center-to-center distance of 13 μ m. The film is patterned in a square with 1 mm sides, and the antenna extends across the middle of the square. The spin wave excited by the antenna can be treated as 1-D propagation in a continuous film because the propagation length is much shorter than the dimensions of the sample. The

^{a)} Author to whom correspondence should be addressed. Electronic mail: elaineli@physics.utexas.edu.

device was placed in an in-plane static magnetic field parallel to the antenna with a strength of 1000 ± 50 Oe measured with a Gaussmeter. The MSSWs are excited by the antenna and propagate away from it, as illustrated in Fig. 1. Using the micro-BLS technique described in Ref. 12, we measured the time-averaged spin wave intensity as a function of distance from the antenna.

To determine the frequency range over which spin waves can be excited effectively, the antenna response was first measured by recording the BLS intensity $1 \mu\text{m}$ from the edge of the antenna as the frequency was scanned from 9 to 11 GHz. The frequency response is shown in Fig. 2(a). For this film thickness, only a single surface mode (i.e., $n=0$ mode) is excited by the microwave source. Higher order modes in the thickness direction are not excited in the frequency range investigated. The response function measured using the BLS intensity near the antenna does not exactly coincide with the amount of power transferred from the antenna into spin waves since the spatial intensity pattern varies with the excitation frequency. Nevertheless, the approximate response function presented in Fig. 2(a) allowed us to choose a reasonable scan range from 9.8 GHz to 10.5 GHz in steps of 0.1 GHz.

At 9.8 and 9.9 GHz, propagating spin waves were not excited and the intensity of the measured magnetization decayed monotonically because these frequencies are below the ferromagnetic resonance (FMR) frequency. The spatial intensity pattern on a logarithmic scale at 9.8 GHz is shown in Fig. 2(b). The spatial dependence can be modeled using a function of the form $C \text{Log}\left(\frac{x}{x+a}\right) + T$, where the parameter a determines how quickly the intensity falls off with distance, and T is the background due to thermal spin waves. Fitting this form to the pattern obtained at 9.8 GHz yields $a = 29 \mu\text{m}$ and $T = 160$ in the arbitrary units for the BLS intensity used in the figures. The spatial dependence of the spin wave intensity measured at 9.9 GHz has approximately the same functional form as that measured at 9.8 GHz, which motivates us to apply the same logarithmic function as the background magnetization in the fits of the spin wave intensity patterns above the FMR frequency, as discussed below.

The measured spin wave intensities as a function of distance from the edge of the antenna at several frequencies near the antenna resonance are shown in Fig. 3. The intensity of the excited MSSW is expected to decay exponentially away from the antenna. However, the observed spatial dependence is much more complicated. At frequencies above

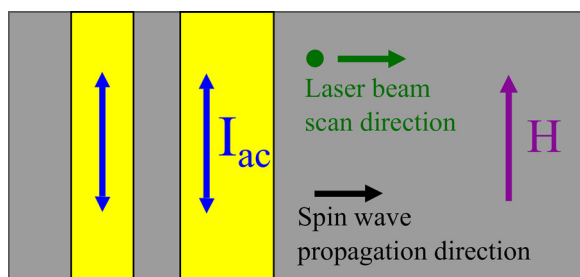


FIG. 1. Illustration of the measured device and experimental configuration. A microwave current is driven through the asymmetric coplanar waveguide to excite spin waves, which propagate away from the antenna.

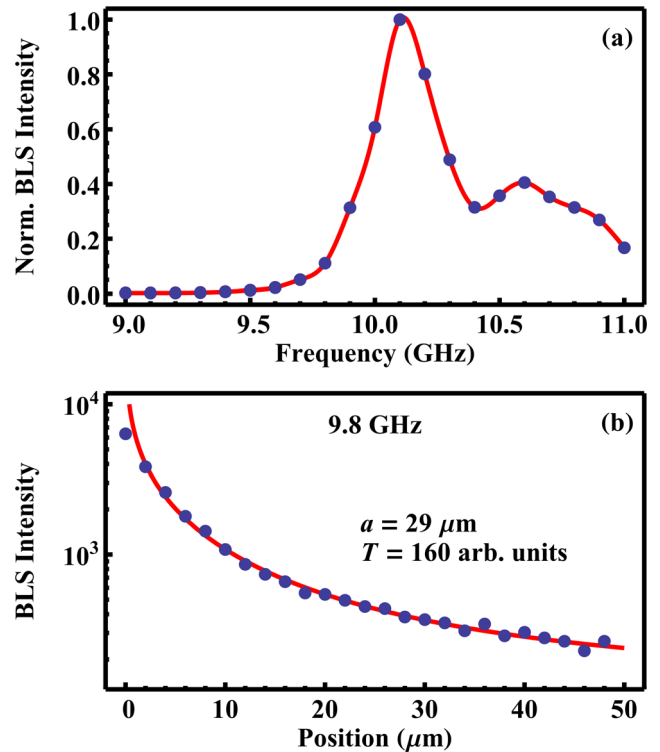


FIG. 2. Part (a) shows the spin wave intensity measured at a point $1 \mu\text{m}$ from the edge of the antenna as a function of frequency. The data points are shown in blue and the red line is only an interpolation to guide the eye. The peak indicates the resonance condition of the antenna with the spin wave response. A spatial scan taken below resonance at 9.8 GHz is shown in (b). The data points are shown in blue and the red line shows the fit to the logarithmic function described in the text.

10.2 GHz, a clear oscillatory behavior was observed in the spatial intensity patterns shown in Figs. 3(a)–3(d). The oscillations can be modeled as the interference between a propagating spin wave and a background magnetization. In contrast to the propagating MSSW with quickly decaying amplitude, this background magnetization has a constant phase and slowly decaying amplitude.

We used the closed-form formula,

$$I_{BLS} \propto \langle m_z(x) \rangle^2$$

$$\propto \left| A \left(\exp\left(ikx - \frac{x}{\Lambda}\right) + \frac{1}{b} \exp(i\phi) \text{Log}\left(\frac{x}{x+a}\right) \right) \right|^2 + T, \quad (1)$$

to fit the spatial intensity patterns at 10.0 GHz and above. The variables in bold font are the fitting parameters. We only consider the perpendicular component of the magnetization since it dominates the BLS signal particularly at small angles of incident light in our experiments.¹⁴ The first term in the sum represents the propagating MSSW with a wave vector k and propagation length Λ . The second term represents the contribution of the background magnetization with the logarithmic functional form determined by fitting the data presented in Fig. 2(b). The parameters ϕ and b , respectively, account for the phase and amplitude differences between the background magnetization and the spin wave. The constant background T is due to the signal from the thermal spin waves and was determined by fitting the spatial intensity pattern in Fig. 2(b).

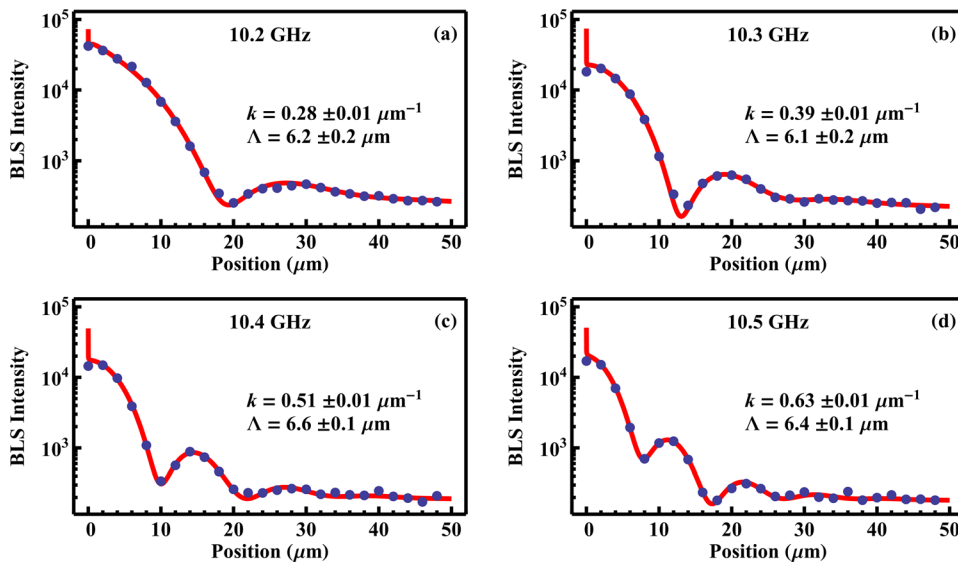


FIG. 3. Log-linear plot of the measured BLS intensity as a function of the propagation distance (measured from edge of the antenna) for several frequencies as indicated. Simple exponential decay was not observed at any frequency. The blue points mark the measured BLS intensity and the red lines indicate the fit result.

The proposed model provides excellent fits to the measurement and accurately reproduces the oscillations, as shown in Figs. 3(a)–3(d). The fitting procedure converged well when a clear dip was observed in the data. Otherwise, the extracted wave vector has large errors, which leads to uncertainty in the other parameters. The key parameter, the spin wave propagation length Λ , was extracted with small errors above 10.2 GHz. For small wave vectors, a simple exponential fit will suffice to extract the propagation length, but for larger wave vectors the interference model is required.

To confirm that the wave vectors extracted from the fits are accurate, we compare the measured dispersion relation with a calculated dispersion relation¹⁵

$$\omega^2 = \gamma^2 [(H_{ext} + 2\pi M_S)^2 - (2\pi M_S)^2 \exp(-2kL)] \quad (2)$$

using parameters extracted from independent measurements. Here, γ is the gyromagnetic ratio (2.93 MHz/Oe) and $H_{ext} = 1,000$ Oe is the measured external magnetic field. The saturation magnetization M_S and Py layer thickness L were extracted by fitting the BLS spectra of thermal spin wave spectra as a function of the applied field (data not shown). These measurements gave $4\pi M_S = 10,600$ Oe and $L = 36$ nm, using an exchange constant of 1.05×10^{-6} erg/cm.¹⁶ The saturation magnetization found for Py is consistent with other values found in the literature, which range between 9 and 11 kOe.^{11,17,18} Figure 4(a) shows the calculated dispersion curve together with the values extracted from the spatial intensity patterns with our model. The agreement of the extracted wave vector with those predicted from the independently calculated dispersion relation is excellent except at 10.0 GHz, where the wavelength is too long for the fitting procedure to converge well.

The dispersion relation allowed us to extract the group velocity for spin waves, which in turn, was used to calculate the propagation length via the simple relation

$$\Lambda_{calc} = \frac{v_g}{\alpha \gamma (H_{ext} + 2\pi M_S)}. \quad (3)$$

The propagation length is expected to be independent of frequency for Damon-Eshbach waves in Py with the large

wavelengths relevant in our experiments.¹⁹ Assuming a damping constant of $\alpha = 0.0074$, consistent with other measurements,^{11,20,21} the predicted propagation length using Eq. (3) is $6.4 \mu\text{m}$. This calculated propagation length agrees well with the experimental values except at the two lowest frequencies where the wave vector could not be determined accurately.

To further confirm the validity of the applied model, we performed additional measurements on the same sample

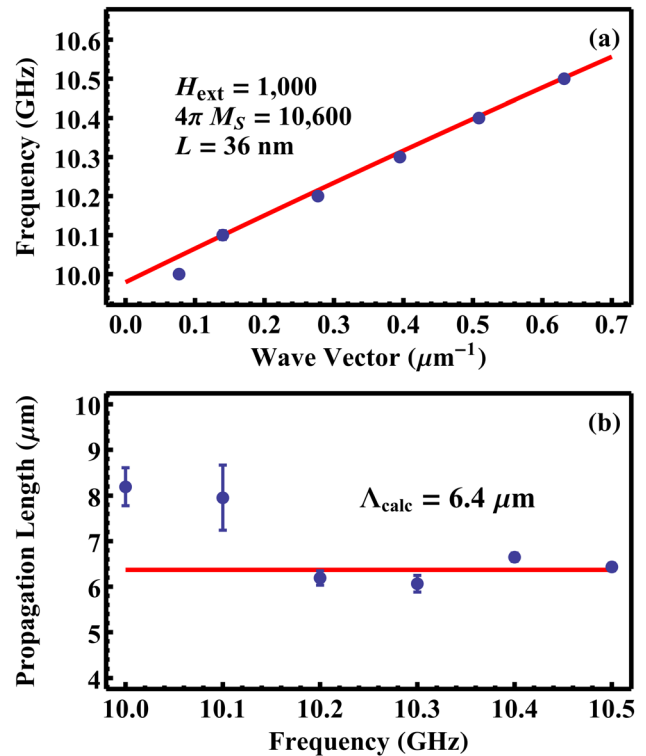


FIG. 4. (a) Experimentally determined dispersion relation (blue dots). The wave vector of the spin wave at a particular frequency was extracted from fit to the closed-form model. The red line represents the calculated dispersion curve using the parameters mentioned in the text. (b) Experimentally determined spin wave propagation lengths (blue dots). The red line indicates the propagation length estimated using Eq. (3).

using spatially resolved ferromagnetic resonance scanning Kerr effect microscopy (SRFMR-SKEM), which measures the amplitude and phase of the excited magnetization.²² In the SRFMR-SKEM experiments, the observed dynamic magnetization is consistent with the micro-BLS measurements: when exciting above the FMR frequency, oscillatory behavior in the intensity is observed, and below FMR, the amplitude decays monotonically away from the antenna. Below FMR, the phase is constant, which confirms our previous claim that no propagating spin waves were excited in Fig. 2(b). Above FMR, the phase of the spin wave advances linearly as it propagates away from the antenna. However, at a distance far from the antenna, the oscillations disappear and the phase becomes constant, which is consistent with our model that includes a quickly decaying spin wave and a slowly decaying background magnetization with uniform phase.

The interference between the propagating spin wave with a background magnetization should be a common phenomenon. We performed numerical calculations following Eq. (36) in Ref. 23 and reproduced our experimental observation qualitatively. The calculations yield the background magnetization below the FMR frequency and the appearance of oscillatory signal upon the excitation of propagation spin waves. The calculations also show that the oscillations appear even with an infinitely thin excitation source, indicating that the oscillations are not a property of the antenna geometry, but rather a property of the magnetic susceptibility. We speculate why the oscillatory behavior has not been observed clearly and discussed explicitly until now. In Ref. 22, the thickness of the Py film was 100 nm, which leads to a much higher MSSW group velocity and thus a longer propagation length than in our case. Therefore, the background magnetization was always weaker than the propagating the spin wave in the range measured. Furthermore, in confined structures, the interference pattern may be obscured by oscillations caused by other mechanisms such as mode beating²⁴ and reflections from edges and inhomogeneities.²⁵ Additionally, this effect may not be apparent in YIG where the spin wave propagation length is hundreds of times longer than that in Py. If the propagation length is long enough, the amplitude of the background magnetization may only become comparable to the spin wave amplitude far from the antenna at which point the spin wave intensity could be too weak to be measured.

In summary, we have shown that the spatial intensity pattern of spin waves radiating from an antenna in a 1-D geometry is not necessarily simple exponential decay. Oscillations in the intensity pattern may arise for excitations above the FMR frequency. The oscillations can be modeled effectively as a propagating spin wave, with a wave vector given by the dispersion relation, that decays exponentially and a

slowly decaying background magnetization with spatially uniform phase. Using a closed-form expression, we were able to extract values for the spin wave propagation length and wave vectors from the observed intensity patterns. The accuracy of these values is confirmed by comparing them with independently calculated expressions.

We gratefully acknowledge financial support from the following sources: AFOSR FA9550-08-1-0463, AFOSR FA-9550-08-1-0058, and the Alfred P. Sloan Foundation. D.B. acknowledges a fellowship from the NSF-IGERT program via Grant No. DGE-0549417. M.T. is supported in part by NSF Grant DMR 1207577. The work at UCLA was supported by the DARPA program on Non-Volatile Logic, and by the Nanoelectronics Research Initiative (NRI) through the Western Institute of Nanoelectronics (WIN).

- ¹V. V. Kruglyak, S. O. Demokritov, and D. Grundler, *J. Phys. D* **43**, 264001 (2010).
- ²J. A. Katine and E. E. Fullerton, *J. Magn. Mater.* **320**, 1217 (2008).
- ³S. S. P. Parkin, M. Hayashi, and L. Thomas, *Science* **320**, 190 (2008).
- ⁴S. I. Kiselev, J. C. Sankey, I. N. Krivorotov, N. C. Emley, R. J. Schoelkopf, R. A. Buhrman, and D. C. Ralph, *Nature* **425**, 380 (2003).
- ⁵W. Rippard, M. Pufall, S. Kaka, S. Russek, and T. J. Silva, *Phys. Rev. Lett.* **92**, 027201 (2004).
- ⁶A. Khitun and K. L. Wang, *Superlattices Microstruct.* **38**, 184 (2005).
- ⁷K.-S. Lee and S.-K. Kim, *J. Appl. Phys.* **104**, 053909 (2008).
- ⁸W. Schilz, Philips Res. Rep. **28**, 50 (1973).
- ⁹M. Bailleul, D. Olligs, C. Fermon, and S. O. Demokritov, *Europhys. Lett.* **56**, 741 (2001).
- ¹⁰M. Bao, K. Wong, A. Khitun, J. Lee, Z. Hao, K. L. Wang, D. W. Lee, and S. X. Wang, *Europhys. Lett.* **84**, 27009 (2008).
- ¹¹W. Hiebert, A. Stankiewicz, and M. Freeman, *Phys. Rev. Lett.* **79**, 1134 (1997).
- ¹²S. O. Demokritov and V. E. Demidov, *IEEE Trans. Magn.* **44**, 6 (2008).
- ¹³R. W. Damon and J. R. Eshbach, *J. Phys. Chem. Solids* **19**, 308 (1961).
- ¹⁴J. Hamrle, J. Pištora, B. Hillebrands, B. Lenk, and M. Münzenberg, *J. Phys. D: Appl. Phys.* **43**, 325004 (2010).
- ¹⁵A. G. Gurevich and G. A. Melkov, *Magnetization Oscillations and Waves* (CRC, 1996).
- ¹⁶N. Smith, D. Markham, and D. LaTourette, *J. Appl. Phys.* **65**, 4362 (1989).
- ¹⁷G. Nahrwold, J. M. Scholtyssek, S. Motl-Ziegler, O. Albrecht, U. Merkt, and G. Meier, *J. Appl. Phys.* **108**, 013907 (2010).
- ¹⁸M. P. Kostylev, A. A. Stashkevich, A. O. Adeyeye, C. Shakespeare, N. Kostylev, N. Ross, K. J. Kennell, R. Magaraggia, Y. Roussigné, and R. L. Stamps, *J. Appl. Phys.* **108**, 103914 (2010).
- ¹⁹D. D. Stancil and A. Prabhakar, *Spin Waves: Theory and Applications* (Springer, 2009).
- ²⁰S. Tamaru, J. Bain, R. van de Veerdonk, T. Crawford, M. Covington, and M. Kryder, *Phys. Rev. B* **70**, 104416 (2004).
- ²¹G. Council, J.-V. Kim, T. Devolder, C. Chappert, K. Shigeto, and Y. Otani, *J. Appl. Phys.* **95**, 5646 (2004).
- ²²S. Tamaru, J. Bain, M. Kryder, and D. Ricketts, *Phys. Rev. B* **84**, 064437 (2011).
- ²³B. A. Kalinikos, *IEE Proc., Part H: Microwaves, Opt. Antennas* **127**, 4 (1980).
- ²⁴V. E. Demidov, S. O. Demokritov, K. Rott, P. Krzysteczko, and G. Reiss, *Appl. Phys. Lett.* **91**, 252504 (2007).
- ²⁵D. R. Birt, B. O'Gorman, M. Tsoi, X. Li, V. E. Demidov, and S. O. Demokritov, *Appl. Phys. Lett.* **95**, 122510 (2009).